Solid Earth Discuss., 7, 1555–1576, 2015
www.solid-earth-discuss.net/7/1555/2015/
doi:10.5194/sed-7-1555-2015

Solid Earth Discussions
Open Access

Experimental study on the electrical conductivity of quartz andesite at high temperature and high pressure: evidence of grain boundary transport

K. S. Hui[1,2], H. Zhang[1], H. P. Li[1], L. D. Dai[1], H. Y. Hu[1], J. J. Jiang[1,2], and W. Q. Sun[1,2]

[1]Key Laboratory of High-Temperature and High-Pressure Study of the Earth's Interior, Institute of Geochemistry, Chinese Academy of Sciences, Guiyang, Guizhou 550002, China
[2]University of Chinese Academy of Sciences, Beijing, 100049, China

Received: 5 April 2015 – Accepted: 13 April 2015 – Published: 6 May 2015

Correspondence to: L. D. Dai (dailidong_2014@hotmail.com)

Published by Copernicus Publications on behalf of the European Geosciences Union.

Abstract

In this study, the grain boundary conductivity of quartz andesite was in situ measured under conditions of 0.5–2.0 GPa and 723–973 K using a YJ-3000t multi-anvil press and Solartron-1260 Impedance/Gain-phase Analyzer. Experimental results indicate that grain interior transport controls the higher frequencies (10^2–10^6 Hz), whereas the grain boundary process dominates the lower frequencies (10^{-1}–10^2 Hz). At a given pressure and temperature range, the relationship between $\log\sigma$ and $1/T$ conforms to an Arrhenius relation. As temperature increased, both of the grain boundary and grain interior conductivities of quartz andesite increased. Under increasing pressure, however, both of the grain boundary and grain interior conductivities of the sample decreased. By the virtue of the dependence of grain boundary conductivity on pressure, the activation enthalpy and the activation volume were calculated at 0.77–1.03 eV and $5.29 \pm 1.94\,\mathrm{cm^3\,mol^{-1}}$, respectively. Furthermore, the small polaron conduction mechanism between the ferrous and ferric ion is also discussed.

1 Introduction

Among the studies of electrical conductivity of rocks at high temperatures and high pressures, grain boundary, similar to temperature and pressure, has been proven a crucial factor that affects the electrical properties of rocks. In particular, the grain boundary which generally exists in rocks has been extensively conducted by more and more researchers. Peridotite, the most important rock in the upper mantle, has been researched to explore the influence of grain boundary on its electrical conductivity in details (Tyburczy and Roberts, 1990; Roberts and Tyburczy, 1991, 1993, 1994; Xu et al., 1998, 2000; ten Grotenhuis et al., 2004; Watson et al., 2010; Wu et al., 2010). However, the function relation between total conductivity, grain boundary, and grain interior conductivity for crustal andesite remains unclear till now.

As a typical representative of calcium alkaline neutral lava which directly contacts with plate subduction, andesite is widely distributed in the orogenic belt around the Pacific Ocean. Extensive studies on the electrical conductivity of andesite have been conducted, and numerous notable results have been achieved. Waff and Weill (1975) measured the electrical conductivities of andesite with different components (Na_2O: 4.96–7.83 wt. % and FeO: 4.99–13.7 wt. %) using a direct current (DC) method at room pressure and different oxygen partial pressures of CO_2 and H_2, and suggested that Alkali ion content significantly impacted the electrical conductivity of andesite. As alkali ion content increased, the electrical conductivity of the sample increased accordingly; this was not dependent on oxygen fugacity or iron content (Waff and Weill, 1975). Later, Tyburczy and Waff (1983) adopted the alternating current (AC) method at pressures of 0–2.55 GPa and temperatures of 1473–1673 K to observe the electrical conductivity of Crater Lake andesite melt. By combining the electrical conductivity data of tholeiite, they concluded that the electrical conductivity of andesite melts increase with the rise of pressure, and that minimum melt faction of 5–10 % can be used to explain the anomalously high electrical conductivity of the upper mantle in typical andesite regions (Tyburczy and Waff, 1983). Recently, Laumonier et al. (2015) measured the electrical conductivity of deictic melts with H_2O content up to 12 wt. % at pressures of 0.15–3.0 GPa and temperatures of 673–1573 K, and demonstrated that the electrical conductivity of dacitic melts is highly dependent on water content. Likewise, the influence of pressure on the activation enthalpy is strongly correlated with its water content. By means of T-P-H_2O model, crustal and mantle wedge conductive bodies have been interpreted by the presence of silica-rich, hydrous, partially crystallized magma (Laumonier et al., 2015). However, previous researches mainly focused on the grain interior conductivity of andesite rather than considered the effect of grain boundary conductivity.

In this study, the grain boundary electrical conductivity of quartz andesite was measured at pressures of 0.5–2.0 GPa, temperatures of 723–973 K and frequency range from 10^{-1} to 10^6 Hz. Then, the characteristic parameters of the electrical conductivity

SED
7, 1555–1576, 2015

of quartz andesite were acquired, including the activation enthalpy and the activation volume. According to these parameters, the relationship between grain interior, grain boundary, and total conductivity was discussed, as well as the conduction mechanism.

2 Experimental procedure

2.1 Sample preparation

The experimental quartz andesite with fresh, un-altered and flesh-yellow in color was collected from Shizhu Town, Yongkang City, Zhejiang Province, China. According to observation under the optical microscope, the sample predominantly consists of fine grained plagioclase, amphibole quartz, and feldspathic matrix, without any accessory mineral phenocrysts.

Before experiment, the quartz andesite was cut into a cylinder with a diameter of 6 mm and height of 6 mm. Then, the cylindrical samples were cleaned in an ultrasonic cleaning device using deionized water, acetone, and ethanol in turn. Finally, the samples were placed into an oven at 323 K for 24 h preparing for experiment. In order to investigate the chemical composition and mineralogical proportion, the sample was determined with X-ray fluorescence spectrometer (XRF) and electron microprobe analysis (EPMA) at the State Key Laboratory of Ore Deposit Geochemistry, Institute of Geochemistry, Chinese Academy of Sciences, Guiyang, China. The results are shown in Table 1.

2.2 High-pressure conductivity cell and impedance measurements

The electrical conductivity in situ measurements at high pressures and high temperatures were performed in the YJ-3000t multi-anvil apparatus and a Solartron-1260 Impedance/Gain-phase Analyzer at the Key Laboratory of High-Temperature and High-Pressure Study of the Earth's Interior, Institute of Geochemistry, Chinese Academy

SED
7, 1555–1576, 2015

of Sciences. A detailed description of the equipment and experimental process were given by Dai et al. (2012) and Hu et al. (2014).

A diagram of the cross-section of high-pressure cell assembly is shown in Fig. 1. In order to avoid the effect of dehydration on the impedance spectroscopy measurement, the pressure medium of pyrophyllite (32.5 mm × 32.5 mm × 32.5 mm) was heated at 1173 K for 12 h in a muffle furnace. The heater is composed of three-layer stainless steel sheets (thickness: 0.5 mm) in the shape of a tube. As in previous studies (Dai et al., 2012; Hu et al., 2014), the alumina and magnesia sleeve were adopted to ensure that the sample was in a relatively insulated environment. A 0.025 mm thickness of nickel foil was placed in the middle of the alumina and magnesia sleeve to shield against external electromagnetic and spurious signal interference. The electrodes were composed of two nickel disks (0.5 mm in thickness and 6 mm in diameter). Besides, temperature was monitored using a NiCr–NiAl thermocouple for the deviation of ±10 K.

During the experiment, the pressure was gone up at the rate of 1.0 GPa h^{-1} to the designated pressure, and then the temperature was increased at the rate of 100 K h^{-1}. Once the temperature reached each preset value, Solartron-1260 Impedance/Gain-phase Analyzer was used to collect the impedance arc with measuring signal voltage of 1 V and frequency of 10^{-1}–10^{6} Hz, characterized by the electrical properties of the sample.

3 Experimental results

In this study, the Nyquist and Bode figures of complex impedance of typical quartz andesite were obtained under conditions of 1.0 GPa, 723–973 K and 10^{-1}–10^{6} Hz (Figs. 2 and 3). From Fig. 2, it is clear that two semicircles displayed characterization of the grain interior and grain boundary impedance of the sample in turn due to the difference relaxation time constant of the impedance arc of grain interior and grain boundary. The semicircle arc crosses the origin and its center falls on the real axis. With the rise of

SED
7, 1555–1576, 2015

temperature, the diameter of impedance arc and value of impedance decrease rapidly, hence the electrical conductivity increases. The Bode plot (Fig. 3) reflects the dependence of modulus ($|Z|$) and phase angle (θ) on frequency. From high to low frequency, the impedance modulus increases rapidly, and the absolute value of the phase angle leans toward zero. According to the impedance spectroscopy theory (Nover et al., 1992; Huebner and Dillenburg, 1995; Huang et al., 2005), the real part (Z'), imaginary part (Z''), modulus ($|Z|$) and phase angle (θ) are expressed as: $Z' = |Z|\cos\theta$ and $Z'' = |Z|\sin\theta$. By means of the series connection of $R_{gi}C_{gi}$ and $R_{gb}C_{gb}$ (R_{gi} and C_{gi}, and as well as R_{gb} and C_{gb} represent the resistance and capacitance that is correspondent to grain interior and grain boundary of sample, respectively), the grain interior and grain boundary resistance were fitted successively. An equivalent circuit composed of a resistor and capacitor in parallel was used simultaneously to fit the total resistance. Furthermore, the grain interior, grain boundary and total electrical conductivity are in accordance with the following expression:

$$\sigma = L/SR, \tag{1}$$

where L is the sample length (m), and S is the cross-sectional area of the electrode (m^2).

At the pressures of 0.5–2.0 GPa and temperatures of 723–973 K, the relationship between electrical conductivity of quartz andesite (σ) and reciprocal temperature ($1/T$) was fitted using the Arrhenius linear relation:

$$\sigma = \sigma_0 \exp(-\Delta H/kT), \tag{2}$$

where σ_0 is the pre-exponential factor ($S\,m^{-1}$), ΔH is the activation enthalpy (eV), k is the Boltzmann constant, and T is the absolute temperature (K). The relationship between activation energy ΔU (eV), pressure P (GPa) and activation volume ΔV ($cm^3\,mol^{-1}$) is expressed as:

$$\Delta H = \Delta U + P \cdot \Delta V. \tag{3}$$

SED
7, 1555–1576, 2015

The grain interior, grain boundary, and total conductivity at different pressure and temperature are plotted against the reciprocal temperature in Figs. 4–6. Figures 4 and 5 show the effect of pressure on the grain interior and grain boundary conductivity, respectively, and the relationship between grain interior, grain boundary and total conductivity at pressure of 1.0 GPa is described in detail in Fig. 6. Furthermore, the ratio of grain interior and grain boundary conductivity dependence on temperature under 1.0 GPa is shown in Fig. 7. In addition, the fitting parameters of the grain interior and grain boundary conductivity are listed in Table 2.

4 Discussions

In the present work, we in situ measured the grain interior (σ_{gi}), grain boundary (σ_{gb}) and total electrical conductivity (σ_t) of quartz andesite at the pressures of 0.5–2.0 GPa and temperatures of 723–973 K. With the rise of pressure, the grain boundary conductivity decreases, while activation enthalpy and pre-exponential factor increase (Fig. 4). From Fig. 6, it is clear that the ground boundary conductivity is higher than either that of grain interior or total conductivity, and that the total conductivity is lower than grain interior conductivity. The relation among grain interior, grain boundary and total conductivity can be described as:

$$\frac{1}{\sigma_t} = \frac{1}{\sigma_{gi}} + \frac{1}{\sigma_{gb}}. \tag{4}$$

The activation energy and activation volume under the experimental conditions are 0.70 ± 0.07 eV and $5.29 \pm 1.94\ cm^3\ mol^{-1}$, respectively. From the ratio of grain boundary to grain interior conductivity at 1.0 GPa can be seen that the tendency of percentage (σ_{gb}/σ_{gi}) gradually increases with increasing temperature, and thus the contribution of grain boundary to the total conductivity of quartz andesite continually increased. Regarding the variation of grain boundary conductivity with pressure, Dai et al. (2008) presented a functional model in which the grain boundary conductivity of peridotite

SED
7, 1555–1576, 2015

varies with grain boundary width. It follows as:

$$\sigma_{\text{gb-micro}} = \sigma_{\text{gb-bulk}}(d/D), \tag{5}$$

where $\sigma_{\text{gb-micro}}$ is microscopic grain boundary conductivity ($\mathrm{S\,m^{-1}}$), $\sigma_{\text{gb-bulk}}$ is the bulk grain boundary conductivity ($\mathrm{S\,m^{-1}}$), d is the grain boundary width (µm), and D is the grain size (µm). In consideration of the above Eq. (5), the diffusivity of cements between feldspar and amphibole in quartz andesite increasing with the rise of pressure results in that the grain boundary width reduces along the direction of the current transmission and the grain conductivity decreases accordingly. The results are consistent with those found by ten Grotenhuis et al. (2004) and Dai et al. (2008) on the effect of pressure on the grain boundary electrical conductivity of peridotite.

From Fig. 5, the grain interior conductivity of quartz andesite decreases with increasing pressure, while the activation enthalpy and pre-exponential factor increase accordingly. Variation in grain interior conductivity dependence on pressure in this study is similar to previous studies which were concentrated on the effect of partially molten of andesite (Waff and Weill, 1975; Tyburczy and Waff, 1983; Laumonier et al., 2015) (Fig. 8). Simultaneously, the activation enthalpy (0.81–1.05 eV) and activation volume ($4.96 \pm 0.52\,\mathrm{cm^3\,mol^{-1}}$) of quartz andesite fall within the same interval as results (0.78–1.17 eV and 3.25–17.9 $\mathrm{cm^3\,mol^{-1}}$, respectively) of Crater Lake andesite obtained by Tyburczy and Waff (1983), and are also close to the values (0.69–1.0 eV and 3.9–24.7 $\mathrm{cm^3\,mol^{-1}}$, respectively) of dacitic melts measured by Laumonier et al. (2015). However, discrepancies in pressure, temperature, melting condition, and chemical composition of the samples are the important influential factors that potentially result in lower values in this study, by 2–3 orders of magnitudes, than previous studies.

On the other hand, the linear relationship between the logarithmic conductivity (Log σ) and reciprocal temperature (T^{-1}) is larger than 99 %, implying that there is only one single dominant conduction mechanism for quartz andesite. On the base of the results, including FeO = 5.02 wt. % in the constituent amphibole in the quartz andesite

SED
7, 1555–1576, 2015

(Table 1), $\Delta H = 0.77$–$1.02\,\mathrm{eV}$ and $\Delta V = 5.29 \pm 1.94\,\mathrm{cm^3\,mol^{-1}}$ (Table 2), we can conclude that the conduction mechanism for quartz andesite is the small polaron which can be used to reasonably explain the variation in grain boundary conductivity. The hopping process can be described as:

$$Fe^{\times}_{Mg} + h^{\cdot} \rightleftharpoons Fe^{\cdot}_{Mg}. \tag{6}$$

In ferromagnesian silicate, the presence of $Fe^{\cdot}_{Mg}$ generating an extra positive charge which repulses cations causing the lattice deformation is small polaron (Dai et al., 2013). As one of the most important conduction mechanism at low temperature region, the conductive characterization of the small polaron is transfer of an electron hole ($h^{\cdot}$) from $Fe^{\cdot}_{Mg}$ to $Fe^{\times}_{Mg}$ (Schmidbauer et al., 2000; Huang et al., 2005; Poe et al., 2008; Dai et al., 2014, 2015; Dai and Karato, 2014a, b). In light of the above mentioned results, the low energy barrier during the transmission process results in the low activation enthalpy of quartz andesite. Besides, another two influential factors including oxygen fugacity and iron content are also affecting the small polaron conduction of quartz andesite. The percentage of ferric iron in the total iron ($Fe^{3+}/\Sigma Fe$) increases with increasing oxygen fugacity; with the rise of iron content, the charge carrier concentration also increases. However, the effect of oxygen fugacity and iron content on the grain boundary conductivity of quartz andesite yet requires further research.

5 Conclusions

At pressures of 0.5–2.0 GPa, temperatures of 723–973 K, and 10^{-1}–10^{6} Hz in frequencies, the grain boundary conductivity of quartz andesite ranges from $10^{-4.8}$–$10^{-2.6}\,\mathrm{S\,m^{-1}}$, the activation enthalpy is 0.77–1.03 eV, and the activation volume is $5.29 \pm 1.94\,\mathrm{cm^3\,mol^{-1}}$, respectively. As a certain function relation of pressure, temperature, and frequency, the grain boundary conductivity increases dramatically and its effect on the total conductivity increases with the rise of temperature. The grain

SED
7, 1555–1576, 2015

boundary conductivity tends to decrease with increasing pressure. At 1.0 GPa, the total conductivity of quartz andesite is approximately one time lower than grain interior conductivity due to the presence of grain boundary. Based on these obtained physical parameters, plus the chemical composition and mineralogical proportion of quartz andesite, altogether suggest that the conduction mechanism of the sample is the small polaron (directional migration of an electron hole ($h^{\cdot}$) from $Fe^{\cdot}_{Mg}$ to $Fe^{\times}_{Mg}$).

The Supplement related to this article is available online at doi:10.5194/sed-7-1555-2015-supplement.

Acknowledgements. This research was financially supported by the "135" Program of Institute of Geochemistry of CAS, Hundred Talents Program of CAS and NSF of China (41474078, 41304068 and 41174079).

References

Dai, L. D. and Karato, S.: Influence of FeO and H on the electrical conductivity of olivine, Phys. Earth Planet. In., 237, 73–79, 2014a.

Dai, L. D. and Karato, S.: High and highly anisotropic electrical conductivity of the asthenosphere due to hydrogen diffusion in olivine, Earth Planet. Sc. Lett., 408, 79–86, 2014b.

Dai, L. D., Li, H. P., Hu, H. Y., and Shan, S. M.: Experimental study of grain boundary electrical conductivities of dry synthetic peridotite under high-temperature, high-pressure, and different oxygen fugacity conditions, J. Geophys. Res., 113, B12211, doi:10.1029/2008JB005820, 2008.

Dai, L. D., Li, H. P., Hu, H. Y., Shan, S. M., Jiang, J. J., and Hui, K. S.: The effect of chemical composition and oxygen fugacity on the electrical conductivity of dry and hydrous garnet at high temperatures and pressures, Contrib. Mineral. Petr., 163, 689–700, 2012.

Dai, L. D., Li, H. P., Hu, H. Y., Jiang, J. J. Hui, K. S., and Shan, S. M.: Electrical conductivity of $Alm_{82}Py_{15}Grs_{3}$ almandine-rich garnet determined by impedance spectroscopy at high temperatures and high pressures, Tectonophysics, 608, 1086–1093, 2013.

Dai, L. D., Li, H. P., Hu, H. Y., Jiang, J. J., and Hui, K. S.: Influence of temperature, pressure, and chemical composition on the electrical conductivity of granite, Am. Mineral., 99, 1420–1428, 2014.
Dai, L. D., Li, H. P., Hu, H. Y., Hui, K. S., Jiang, J. J., Li, J., and Sun, W. Q.: Electrical conductivity of gabbro: the effect of temperature, pressure and oxygen fugacity, Eur. J. Mineral., 27, 215–224, 2015.
Hu H. Y., Dai, L. D., Li, H. P., Jiang, J. J., and Hui, K. S.: Electrical conductivity of K-feldspar at high temperature and high pressure, Miner. Petrol., 108, 609–618, 2014.
Huang, X. G., Xu, Y. S., and Karato, S.: Water content in the transition zone from electrical conductivity of wadsleyite and ringwoodite, Nature, 434, 746–749, 2005.
Huang, X. G., Huang, X. G., and Bai, W. M.: Progress of high temperature and high pressure experimental study on the electrical conductivity of the minerals and rocks (in Chinese), Prog. Geophys., 25, 1247–1258, 2010.
Huebner, J. S. and Dillenburg, R. G.: Impedance spectra of hot, dry silicate minerals and rock-qualitative interpretation of spectra, Am. Mineral., 80, 46–64, 1995.
Laumonier, M., Gaillard, F., and Sifre, D.: The effect of pressure and water concentration on the electrical conductivity of dacitic melts: implication for magnetotelluric imaging in subduction areas, Chem. Geol., doi:10.1016/j.chemgeo.2014.09.019, online first, 2015.
Nover, G., Will, G., and Waitz, R.: Pressure-induced phase-transition in Mg_2GeO_4 as determined by frequency-dependent complex electrical-resistivity measurements, Phys. Chem. Miner., 19, 133–139, 1992.
Poe, B. T., Romano, C., Varchi, V., Misiti, V., and Scarlato, P.: Electrical conductivity of a phonotephrite from Mt. Vesuvius: the importance of chemical composition on the electrical conductivity of silicate melts, Chem. Geol., 256, 193–202, 2008.
Roberts, J. J. and Tyburczy, J. A.: Frequency dependent electrical properties of polycrystalline olivine compacts, J. Geophys. Res., 96, 16205–16222, 1991.
Roberts, J. J. and Tyburczy, J. A.: Frequency-dependent electrical-properties of dunite as functions of temperature and oxygen fugacity, Phys. Chem. Miner., 19, 545–561, 1993.
Roberts, J. J. and Tyburczy, J. A.: Frequency-dependent electrical-properties of minerals and partial-melts, Surv. Geophys., 15, 239–262, 1994.
Schmidbauer, E., Kunzmann, T., Fehr, T., and Hochleitner, R.: Electrical resistivity and Fe-57 Mossbauer spectra of Fe-bearing calcic amphiboles, Phys. Chem. Miner., 27, 347–356, 2000.

SED
7, 1555–1576, 2015

Experimental study on the electrical conductivity of quartz andesite

K. S. Hui et al.

Title Page
Abstract Introduction
Conclusions References
Tables Figures
Back Close
Full Screen / Esc
Printer-friendly Version
Interactive Discussion

ten Grotenhuis, S. M., Drury, M. R., Peach, C. J., and Spiers, C. J.: Electrical properties of fine-grained olivine: evidence for grain boundary transport, J. Geophys. Res., 109, B06203, doi:10.1029/2003JB002799, 2004.

Tyburczy, J. A. and Roberts, J. J.: Low frequency electrical response of polycrystalline olivine compacts: grain boundary transport, Geophys. Res. Lett., 17, 1985–1988, 1990.

Tyburczy, J. A. and Waff, H. S.: Electrical conductivity of molten basalt and andesite to 25 kilobars pressure: geophysical significance and implications for charge transport and melt structure, J. Geophys. Res., 88, doi:10.1029/JB088iB03p02413, 1983.

Waff, H. S. and Weill, D. F.: Electrical conductivity of magmatic liquids effects of temperatureeffects of temperature, oxygen fugacity and composition, Earth Planet. Sc. Lett., 28, 254–260, 1975.

Watson, H. C., Roberts, J. J., and Tyburczy, J. A.: Effect of conductive impurities on electrical conductivity in polycrystalline olivine, Geophys. Res. Lett., 37, L02302, doi:10.1029/2009GL041566, 2010.

Wu, X. P., Zhang, B. H., Xu, J. S., Katsura, T., Zhai, S. M., Yoshino, T., Manthilake, G., and Shatskiy, A.: Electrical conductivity measurements of periclase under high pressure and high temperature, Phys. B, 405, 53–56, 2010.

Xu, Y. S., Poe, B. T., Shankland, T. J., and Rubie, D. C.: Electrical conductivity of olivine, wadsleyite, and ringwoodite under upper-Mantle conditions, Science, 280, 1415–1418, 1998.

Xu, Y. S., Shankland, T. J., and Duba, A. G.: Pressure effect on electrical conductivity of mantle olivine, Phys. Earth Planet. In., 118, 149–161, 2000.

SED
7, 1555–1576, 2015

Experimental study on the electrical conductivity of quartz andesite

K. S. Hui et al.

Table 1. Whole rock analysis by X-ray fluorescence (XRF) and chemical composition of dominant minerals for quartz andesite by the electron microprobe (EPMA).

Oxides	XRF for whole rock (wt. %)	EPMA for Anorthoclase (wt. %)	EPMA for Albite (wt. %)	EPMA for Amphibole (wt. %)
SiO_2	66.47	59.56	65.25	52.47
Al_2O_3	13.57	26.20	19.75	3.61
MgO	0.44	0.15	0.03	15.72
CaO	1.12	2.28	0.62	12.18
Na_2O	4.98	6.99	10.55	0.20
K_2O	4.16	3.09	0.02	0.18
FeO	5.02	0.90	1.03	11.23
TiO_2	0.22	0.03	0.01	0.33
Cr_2O_3	0.02	0.02	1.47	0.03
MnO_2	–	0.04	0.00	0.12
P_2O_5	0.81	–	–	–
L.O.I	2.74	–	–	–
Total	99.55	99.26	98.73	96.07

SED
7, 1555–1576, 2015

Table 2. Fitted parameters for the grain interior and grain boundary conductivity of quartz andesite.

	P (GPa)	T (K)	Log σ_0 (S m^{-1})	ΔH (eV)	γ^2	ΔU (eV)	ΔV (cm^3 mol^{-1})
Grain boundary	0.5	723–973	1.44	0.77	99.13	0.70 ± 0.07	5.29 ± 1.94
	1.0	723–973	1.66	0.87	99.69		
	1.5	723–973	2.43	1.03	99.70		
	2.0	723–973	1.85	0.97	99.83		
Grain interior	0.5	723–973	1.63	0.81	99.97	0.76 ± 0.06	4.96 ± 0.52
	1.0	723–973	1.90	0.93	99.99		
	1.5	723–973	2.41	1.05	99.81		
	2.0	723–973	2.03	1.02	99.70		

SED
7, 1555–1576, 2015

Experimental study on the electrical conductivity of quartz andesite

K. S. Hui et al.

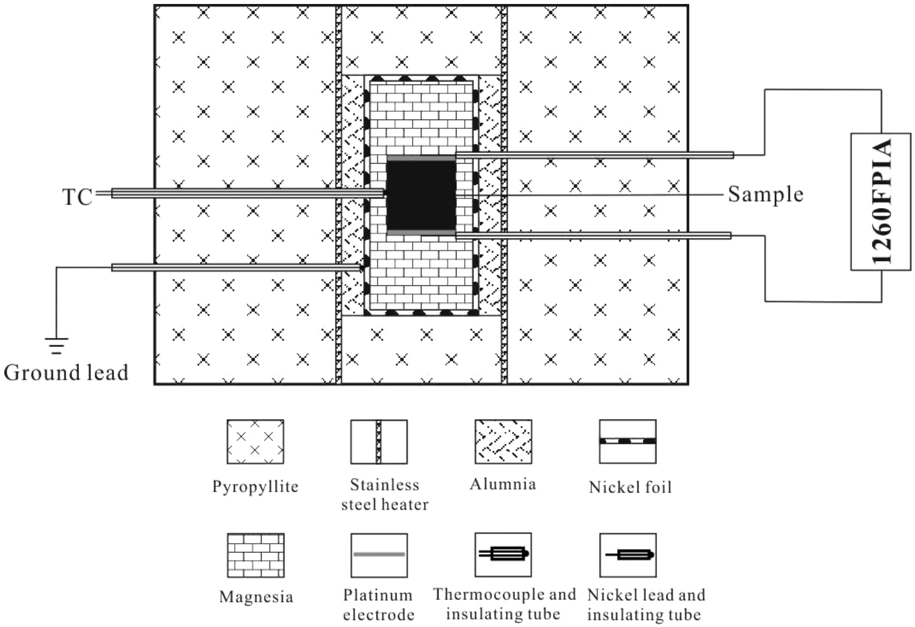

Figure 1. Experimental setup of electrical conductivity measurements.

SED
7, 1555–1576, 2015

Experimental study on the electrical conductivity of quartz andesite

K. S. Hui et al.

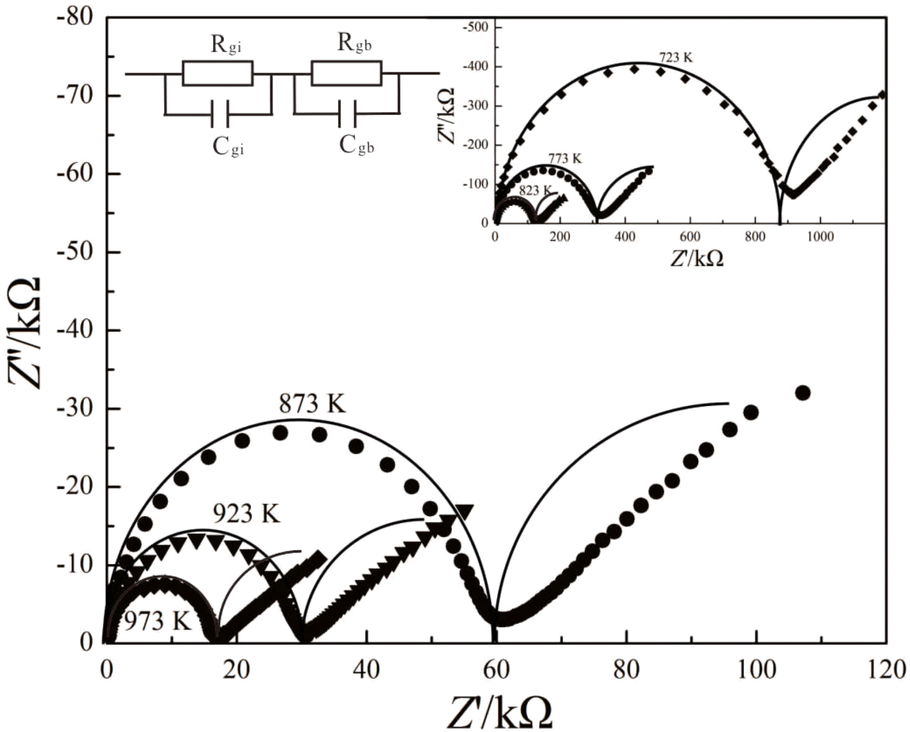

Figure 2. Nyquist plot of the complex impedance of quartz andesite under conditions of 1.0 GPa and 723–973 K.

SED
7, 1555–1576, 2015

Experimental study on the electrical conductivity of quartz andesite

K. S. Hui et al.

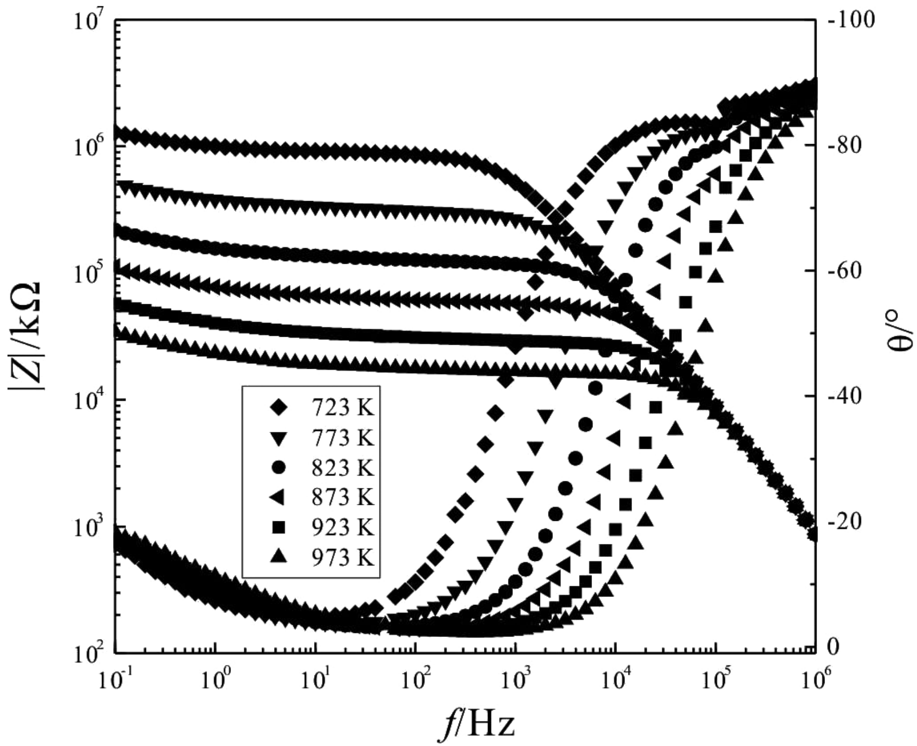

Figure 3. Bode plot of dependence of modulus and phase angle on frequency quartz andesite under conditions of 1.0 GPa and 723–973 K.

SED
7, 1555–1576, 2015

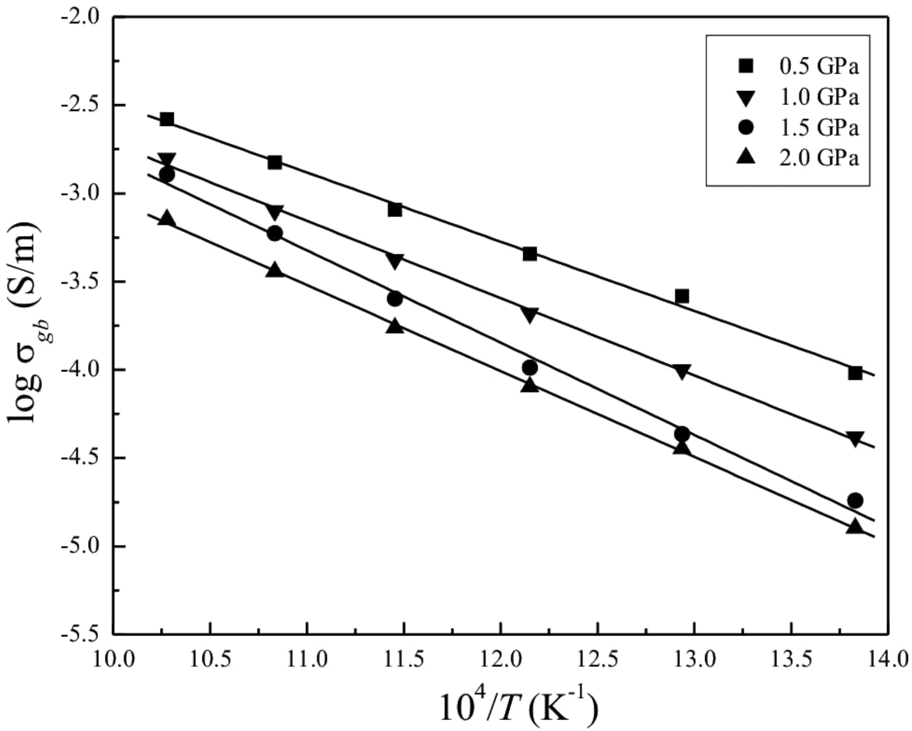

Figure 4. The relationship of the logarithmic grain boundary conductivity vs. reciprocal temperature under conditions of 0.5–2.0 GPa and 723–973 K.

SED
7, 1555–1576, 2015

Experimental study on the electrical conductivity of quartz andesite

K. S. Hui et al.

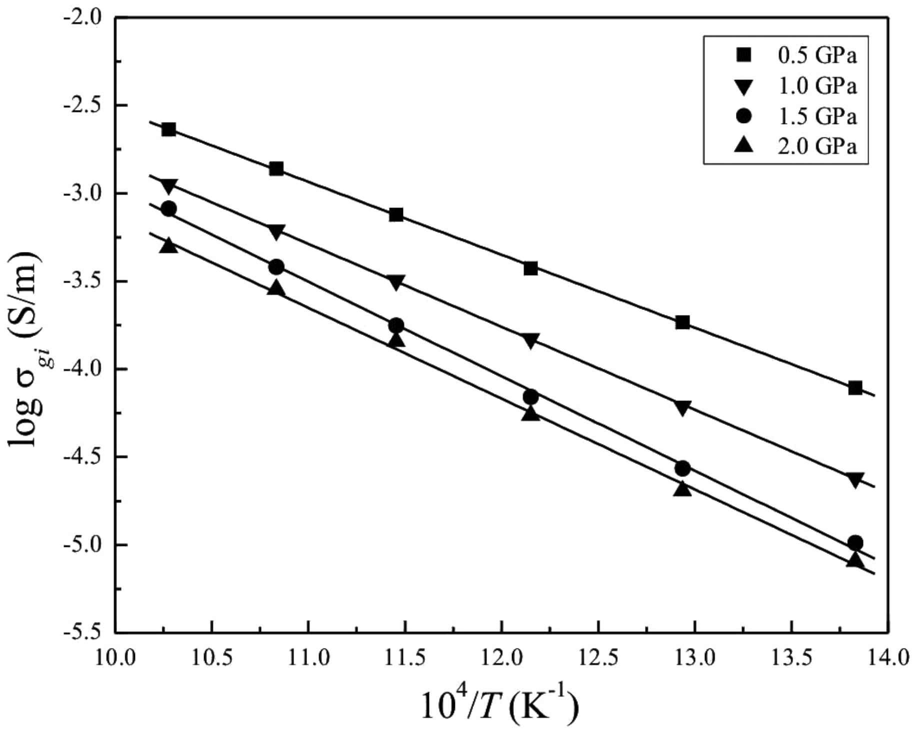

Figure 5. The relationship of the logarithmic grain interior conductivity vs. reciprocal temperature under conditions of 0.5–2.0 GPa and 723–973 K.

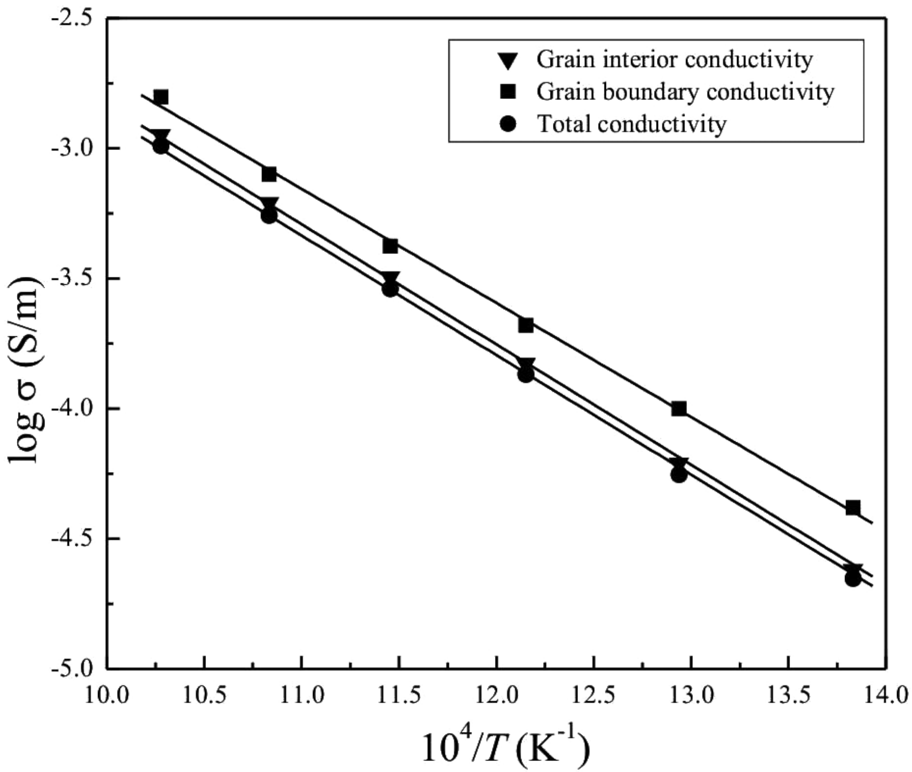

Figure 6. The relationship of grain interior, grain boundary and total conductivity under conditions of 1.0 GPa and 723–973 K.

SED
7, 1555–1576, 2015

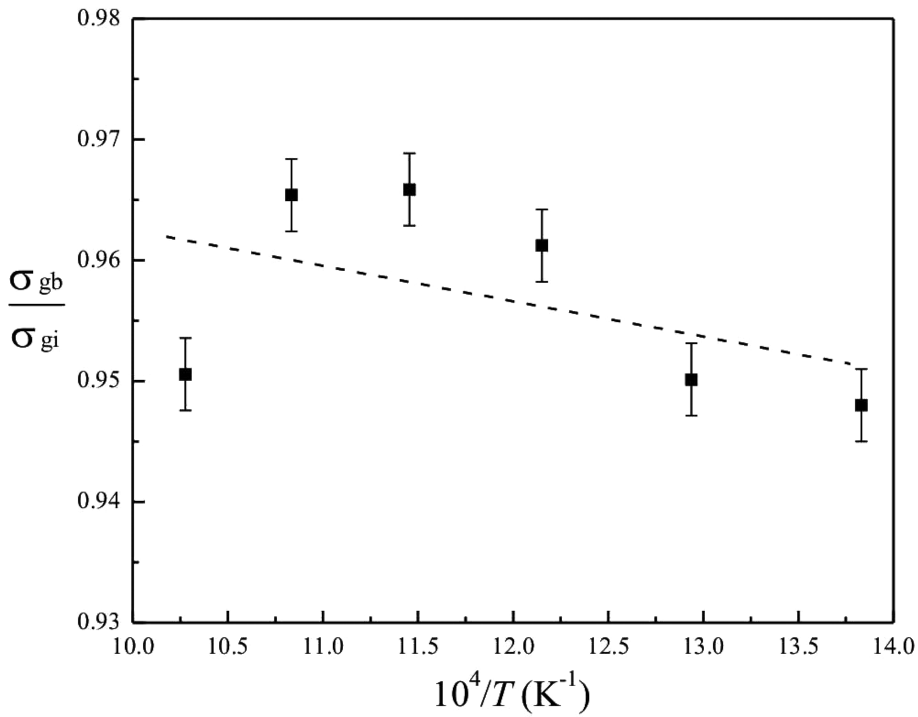

Figure 7. The relationship of grain boundary/grain interior conductivity (σ_{gb}/σ_{gi}) vs. reciprocal temperature ($1/T$) under conditions of 1.0 GPa and 723–973 K.

SED
7, 1555–1576, 2015

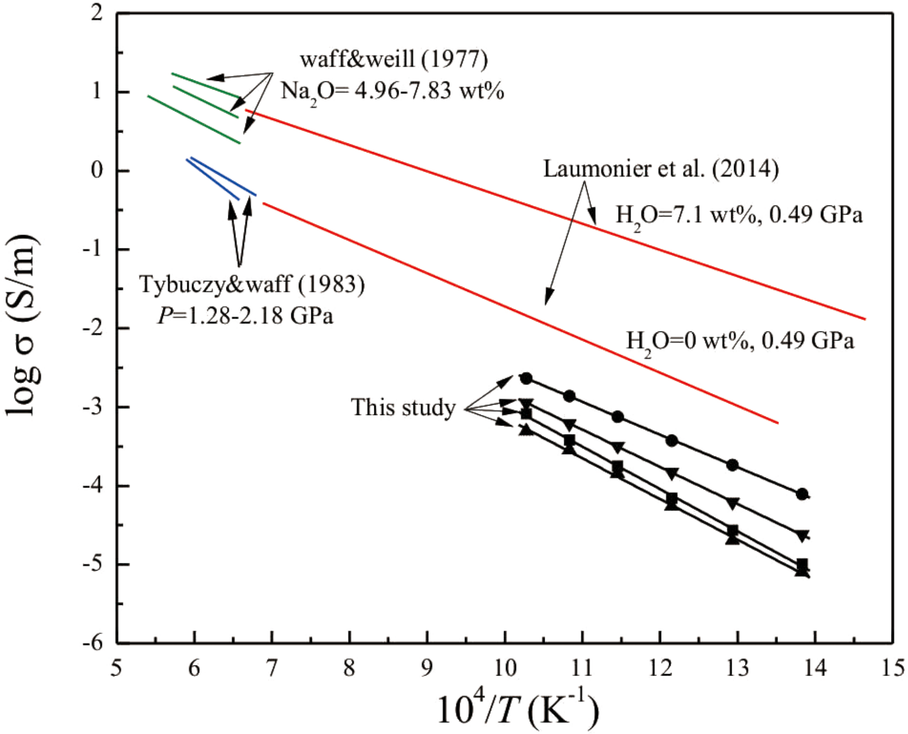

Figure 8. A comparison of grain interior conductivity of quartz andesite with previous studies.